Cellular/Molecular

Transcription Factor CREB3L1 Regulates Vasopressin Gene Expression in the Rat Hypothalamus

Mingkwan Greenwood,[1] Loredana Bordieri,[1] Michael P. Greenwood,[1] Mariana Rosso Melo,[2] Debora S. A. Colombari,[2] Eduardo Colombari,[2] Julian F. R. Paton,[3] and David Murphy[1,4]

[1]School of Clinical Sciences, University of Bristol, Bristol BS1 3NY, United Kingdom, [2]Department of Physiology and Pathology, School of Dentistry, São Paulo State University, Araraquara, São Paulo 14801-385, Brazil, [3]School of Physiology and Pharmacology, University of Bristol, Bristol BS8 1TD, United Kingdom, and [4]Department of Physiology, University of Malaya, Kuala Lumpur 50603, Malaysia

Arginine vasopressin (AVP) is a neurohypophysial hormone regulating hydromineral homeostasis. Here we show that the mRNA encoding cAMP responsive element-binding protein-3 like-1 (CREB3L1), a transcription factor of the CREB/activating transcription factor (ATF) family, increases in expression in parallel with AVP expression in supraoptic nuclei (SONs) and paraventicular nuclei (PVNs) of dehydrated (DH) and salt-loaded (SL) rats, compared with euhydrated (EH) controls. In EH animals, CREB3L1 protein is expressed in glial cells, but only at a low level in SON and PVN neurons, whereas robust upregulation in AVP neurons accompanied DH and SL rats. Concomitantly, CREB3L1 is activated by cleavage, with the N-terminal domain translocating from the Golgi, via the cytosol, to the nucleus. We also show that CREB3L1 mRNA levels correlate with AVP transcription level in SONs and PVNs following sodium depletion, and as a consequence of diurnal rhythm in the suprachiasmatic nucleus. We tested the hypothesis that CREB3L1 activates AVP gene transcription. Both full-length and constitutively active forms of CREB3L1 (CREB3L1CA) induce the expression of rat AVP promoter-luciferase reporter constructs, whereas a dominant-negative mutant reduces expression. Rat AVP promoter deletion constructs revealed that CRE-like and G-box sequences in the region between −170 and −120 bp are important for CREB3L1 actions. Direct binding of CREB3L1 to the AVP promoter was shown by chromatin immunoprecipitation both *in vitro* and in the SON itself. Injection of a lentiviral vector expressing CREB3L1CA into rat SONs and PVNs resulted in increased AVP biosynthesis. We thus identify CREB3L1 as a regulator of AVP transcription in the rat hypothalamus.

Key words: **CREB3L1; hyperosmotic stress; hypothalamus; transcription; vasopressin**

Introduction

Arginine vasopressin (AVP) is a neurohypophysial hormone that plays an important role in hydromineral homeostasis (Antunes-Rodrigues et al., 2004). AVP is synthesized in magnocellular neurons (MCNs) of the supraoptic nuclei (SONs) and the paraventricular nuclei (PVNs) of the hypothalamus and is transported to the posterior pituitary, where it is stored until released into the general circulation in response to hyperosmotic stressors, such as dehydration (DH; complete fluid deprivation for 3 d) or salt loading (SL; obligate consumption of 2% w/v NaCl for 7 d). Increased plasma osmolality is sensed by specialized osmoreceptor neurons in the circumventricular organs (McKinley et al., 2003) that project to the SONs and PVNs (Miselis, 1981). Excitatory signals evoke AVP release (Bourque, 2008), which acts at the level of the kidney to conserve water (Boone and Deen, 2008). AVP is also expressed in the hypothalamic suprachiasmatic nucleus (SCN), where it is regulated by circadian cues (Uhl and Reppert, 1986).

A transcriptionally mediated increase in AVP gene expression accompanies chronic hyperosmotic stress (Murphy and Carter, 1990), but the mechanisms are not fully understood. It is known that cAMP levels increase in the rat SON following SL, and this is thought to stimulate AVP expression (Carter and Murphy, 1989; Ceding et al., 1990) through the activation of the protein kinase A pathway and subsequent cAMP responsive element-binding protein (CREB) phosphorylation (Shiromani et al., 1995). The immediate early genes, Fos/Jun family proteins have also been implicated in the induction of AVP transcription through binding at an activator protein-1 element (Carter and Murphy, 1990; Luckman et al., 1996). Reporter assays certainly indicated that CREB positively regulates AVP transcription *in vitro* (Iwasaki et al., 1997). However, in recent *in vivo* studies, injecting a recombinant adeno-associated virus expressing a dominant-negative mutant form of CREB into rat SONs, failed to significantly re-

Received Oct. 10, 2013; revised Dec. 9, 2013; accepted Dec. 13, 2013.

Author contributions: M.G., L.B., M.P.G., D.S.A.C., E.C., J.F.R.P., and D.M. designed research; M.G., L.B., M.P.G., and M.R.M. performed research; M.G. and M.P.G. analyzed data; M.G. and M.P.G. wrote the paper.

This research was supported by the Medical Research Council (Grant G0700954, to L.B., DM), Biotechnology and Biological Sciences Research Council (Grant BB/G006156/1, to M.P.G., J.F.R.P., and D.M.; Grant BB/J01515/1, to M.G., J.F.R.P., and D.M.), Fundação de Amparo à Pesquisa do Estado de São Paulo (Temático 2011/50770-1, to E.C. and D.S.A.C.), and the University of Malaya (HIR Award H-20001-E000086, to D.M.). We thank Professor Harold Gainer (National Institute of Neurological Disorders and Stroke, National Institutes of Health) for providing us with antibodies recognizing AVP NP-I and OXT NP-II.

The authors declare no competing financial interests.

This article is freely available online through the *J Neurosci* Author Open Choice option.

Correspondence should be addressed to David Murphy, Dorothy Hodgkin Building, Whitson Street, Bristol BS1 3NY, UK. E-mail: d.murphy@bristol.ac.uk.

DOI:10.1523/JNEUROSCI.4343-13.2014

duce AVP mRNA expression after hyperosmotic stimulation (Lubelski et al., 2012). Thus, clear *in vivo* evidence for a role for CREB in AVP gene transcription is still lacking. Indeed, no principal transcription factor or factors, mediating either basal or osmotically stimulated AVP expression have been identified in MCNs of SONs and PVNs.

We and others have used microarrays to describe transcriptome changes in the rat and mouse SONs and PVNs in response to DH (Mutsuga et al., 2005; Hindmarch et al., 2006; Yue et al., 2006b). Using this approach, we identified a number of upregulated transcription factor transcripts (Qiu et al., 2007; Stewart et al., 2011), one of which encodes CREB3 like-1 (CREB3L1). CREB3L1, also known as OASIS (old astrocyte specifically induced substance), was first identified in long-term cultured mouse astrocytes (Honma et al., 1999). Various functions have been ascribed to CREB3L1 (Murakami et al., 2009; Denard et al., 2011; Saito et al., 2012), but no role for CREB3L1 in hypothalamic neurons has been reported previously. In this study, we characterized the functions of CREB3L1 in the hypothalamus. Using different experimental models, we observed that changes in CREB3L1 expression correlate with AVP expression. We thus tested the hypothesis that CREB3L1 activates AVP gene transcription.

Materials and Methods

Animals. Male Sprague Dawley rats weighing 250–300 g were used in this study, with the exception of the furosemide experiments, which were conducted on male Holtzman rats. The rats were housed at a constant temperature of 22°C and a relative humidity of 50–60% (v/v) under a 14:10 h light/dark cycle. The rats were given free access to food and tap water for at least 1 week before experimentation. To induce hyperosmotic stress, water was removed for 1 or 3 d (DH) or replaced by 2% (w/v) NaCl in drinking water for 1 or 7 d (SL). A single 10 mg/kg, s.c, injection of furosemide versus vehicle injection was used to investigate sodium depletion. In this instance, tap water was replaced with deionized water, and animals were provided with sodium-deficient food (powdered corn meal, 0.001% sodium, and 0.33% potassium) for 24 h. Animal experiments were performed between 10:00 A.M. and 1:00 P.M. with the exception of SCN circadian studies where zeitgeber time 7 (ZT7) was compared with ZT19 (ZT0 = 5:00 A.M., lights on). All experiments were performed under the licencing arrangements of the Animals (Scientific Procedures) Act (1986) with the approval of the local ethics committee.

RNA extraction and cDNA synthesis. The rats were stunned and decapitated, and brains were removed and immediately frozen in powdered dry ice. A 1 mm micropunch (Fine Scientific Tools) was used to collect SON, PVN, and SCN samples from 60 μm coronal sections in a cryostat. Sections were mounted on glass slides, stained with 0.1% (w/v) toluidine blue, then visualized on a light microscope until the desired brain nuclei were visible. Using the optic chiasm (SON and SCN) or neurons medial lateral to the third ventricle (PVN) for reference, samples were punched from frozen brain slices and dispensed into 1.5 ml tubes kept on dry ice within the cryostat. Total RNA was extracted from punch samples by combining Qiazol Reagent with Qiagen's RNeasy kit protocols (Qiagen). The punch samples were removed from dry ice and rapidly resuspended, by vortexing, in 1 ml of Qiazol reagent. Following Qiazol phase separation with chloroform, 350 μl of the upper aqueous phase was removed, mixed with 350 μl of 70% ethanol, and applied to RNeasy columns. The remaining steps were performed as recommended by the manufacturer. For cDNA synthesis, 200 ng of total RNA was reverse transcribed using the Quantitect reverse transcription kit (Qiagen).

Real-time quantitative PCR analysis. Steady-state RNA levels in the SON, PVN and SCN were assessed by quantitative PCR (qPCR). Primers for CREB3L1 (5′-GAGACCTGGCCAGAGGATAC-3′ and 5′-GTCAGT GAGCAAGAGAACGC-3′), total AVP mRNA (5′-TGCCTGCTACTT CCAGAACTGC-3′ and 5′-AGGGGAGACACTGTCTCAGCTC-3′), and AVP heteronuclear RNA (hnRNA) (5′-GAGGCAAGAGGGCCA CATC-3′ and 5′-CTCTCCTAGCCCATGACCCTT-3′) were synthesized by Eurofins MWG Operon, while RPL19, GAPDH, and GFP primers were predesigned by Quantitect Primer assays (Qiagen). The optimization and validation of primers were performed using standard ABI protocols. The cDNA from the reverse transcription reaction was used as a template for subsequent PCRs, which were performed in duplicate. Quantitative PCR was conducted in 25 μl reaction volumes using SYBR Green master mix buffer (Roche) using an ABI 7500 Sequence Detection System. For relative quantification of gene expression the $2^{-\Delta\Delta CT}$ method was used (Livak and Schmittgen, 2001). The internal control gene used for these analyses was the housekeeping gene RPL19, though comparable results were also obtained with 18S and GAPDH.

Protein extraction. Using the optic chiasm as a reference, 1 mm slices containing the hypothalamus were excised using an ice-cold brain matrix, and the SONs and PVNs were dissected. To prepare whole-cell lysates, samples were incubated in RIPA buffer (150 mM NaCl, 50 mM Tris-HCl, pH 7.5, 1% w/v sodium deoxycholate, 0.1% w/v SDS, 1 mM EDTA, 1 mM EGTA, 1% v/v NP-40) containing protease inhibitors (P8340, Sigma) on ice for 30 min, and passed through a 23-gauge syringe needle. The homogenates were centrifuged at 10,000 × *g* for 10 min at 4°C, and the supernatant was stored at −20°C. Cellular localization of proteins (cytoplasmic vs nuclear) was investigated in SON and PVN samples as described previously (Noguchi et al., 2010). Samples were homogenized in 500 μl of S1 buffer (10 mM HEPES, pH 7.9, 10 mM KCl, 1.5 mM $MgCl_2$, 0.1 mM EGTA, pH 7) and centrifuged at 2000 × *g* for 10 min at 4°C. The supernatant, containing cytosolic proteins, was collected and stored at −80°C. The pellet was resuspended in S1 buffer and passed 10 times through a 25-gauge needle, followed by centrifugation at 2000 × *g* for 10 min at 4°C. The pellet was washed again in S1 buffer and resuspended in 1.2 pellet volumes of S2 buffer (10 mM HEPES, pH 7.9, 400 mM NaCl, 1.5 mM $MgCl_2$, 0.1 mM EGTA, pH 7, 5% v/v glycerol). Samples were shaken on ice for 1 h and centrifuged at 22,000 × *g* for 30 min at 4°C. The supernatant, containing nuclear proteins, was collected and stored at −80°C. The S1 and S2 buffers contained protease inhibitors and 0.5 mM DTT. For validation of full-length CREB3L1 (CREB3L1FL) expression, HEK293T cells were transfected by the calcium phosphate method using 2 μg/well plasmid expressing the constitutively active form of CREB3L1 (CREB3L1CA), CREB3L1FL, or pcDNA3. Total proteins were extracted using RIPA buffer at 48 h after transfection. Protein concentration was determined by Bradford assay (Bradford, 1976).

Immunoblotting. Fivefold concentrated Laemmli buffer solution (217 mM Tris, pH 6.8, 10% w/v SDS, 50% v/v glycerol, 1% w/v bromophenol blue) was added to the protein samples in presence of β-mercaptoethanol (10% v/v). Protein samples were heated at 90°C for 10 min, fractionated on 10% SDS polyacrylamide gels, then transferred to PVDF membranes. Membranes were incubated in 10% (w/v) skimmed milk in Tris-buffered saline (150 mM NaCl, 20 mM Tris-HCl, pH 7.6) with 0.1% Tween 20 (TBST) at room temperature for 1 h, followed by incubation with appropriate primary antibody diluted in 10% skimmed milk in TBST at 4°C overnight. After three 10 min washes, the membranes were incubated with appropriate secondary antibody conjugated with horseradish peroxidase for 1 h at room temperature. Membranes then were washed with TBST. Signal was detected using enhanced chemiluminescence ECLPlus reagent (GE Healthcare Biosciences). Immunoblots were stripped in Restore Western blot-stripping buffer (Thermo Scientific) and reprobed to assess multiple proteins on the same blot. The following antibodies were used for immunoblotting: goat anti-C-terminal CREB3L1 antibody (1:500; Abcam), goat anti-N-terminal CREB3L1 antibody (1:500; R&D Systems), goat anti-GAPDH (1:1000; Santa Cruz Biotechnology), or mouse anti-Histone H1 antibody (1:400; Santa Cruz Biotechnology).

Immunohistochemistry and immunofluorescence. Rats were anesthetized with sodium pentobarbitone (100 mg/kg, i.p.) and transcardially perfused with 0.1 M PBS, pH 7.4, followed by 4% (w/v) paraformaldehyde (PFA) in 0.1 M PBS. The brains were removed and postfixed overnight in 4% (w/v) PFA followed by 30% (w/v) sucrose prepared in PBS. Coronal sections (40 μm) of the forebrain were cut on a cryostat, washed in 0.1 M PBS, pH 7.4, treated with 0.3% (v/v) hydrogen peroxide for 30 min, and blocked for 1 h in 10% (v/v) horse serum (Sigma). The sections then were incubated in a goat anti-CREB3L1 antibody (N-terminal;

1:200 in PBS) at 4°C for overnight. The avidin–biotin complex method was used to detect the signal (ABC Elite Kit, Vector Laboratories), and the reaction product was visualized with 3,3-diaminobenzidine (Roche). The sections were mounted onto glass slides with 0.5% gelatin, air dried, then dehydrated through a graded series of ethanol. The sections were cleared in Histo-clear, and coverslipped in DPX mounting media (VWR).

For double-labeling immunofluorescence, tissue samples were prepared using the same method as described for immunohistochemistry. Sections were blocked in 5% horse serum prepared in 0.1 M PBS with 0.25% (v/v) Triton (PBST) for 30 min and then incubated with appropriate primary antibodies at 4°C for 48 h. The sections were washed three times in PBS for 5 min and incubated with 1:500 dilution of appropriate biotinylated secondary antibody in PBST for 1 h at room temperature. The sections were washed three times for 5 min with PBS and incubated for 1 h with Alexa Fluor 488 streptavidin-conjugated and Alexa Fluor 594 donkey anti-mouse or rabbit IgG (Invitrogen). After three washes with PBS, sections were mounted onto glass slides with 0.5% gelatin, and sealed with VectorShields hard mounting media with DAPI (Vector Laboratories). The following antibodies were used for immunostaining: anti-N-terminal CREB3L1 antibody (1:250; R&D Systems); mouse monoclonal antibodies recognizing AVP neurophysin I (NP-I; PS41; 1:100); oxytocin (OXT) NP-II (PS38; 1:100; Ben-Barak et al., 1985); rabbit antibodies for protein disulfide isomerase (PDI; 1:100; Cell Signaling Technology); RCAS1 (1:500; Cell Signaling Technology); or mouse monoclonal anti-glial fibrillary acidic protein (GFAP) (1:400; Millipore).

To test anti-N-terminal CREB3L1 antibody specificity, HEK293T cells were grown on coverslips in 12-well tissue culture plates and transfected, by the calcium phosphate method, with 1 μg/well plasmid expressing CREB3L1FL or pcDNA3. At 48 h after transfection, the cells were fixed with 4% (w/v) PFA for 10 min, washed two times in PBS, and permeabilized in PBST for 10 min. After two washes in PBST, the cells were blocked and incubated with anti-N-terminal CREB3L1 antibody. The remaining steps were performed as described for immunofluorescent staining of tissue slices.

Luciferase assays. Plasmid constructs expressing CREB3L1CA and a dominant-negative mutant of CREB3L1 (CREB3L1DN) of mouse CREB3L1 cloned into pcDNA3 were provided by Kazunori Imaizumi (University of Miyazaki, Miyazaki, Japan). CREB3L1FL was amplified from rat SON cDNA using primers (5′-GGCGCG ATGGACGCCGTCTT-3′ and 5′-GGTCTCGG AGTGGCCTAGGAG-3′) and cloned into the pcDNA3 plasmid. A series of rat AVP promoter luciferase reporter constructs (1 kb, and 350, 170, 120, or 70 bp; Adan and Burbach, 1992) were excised from p19LUC with HindIII (blunted)–SalI and cloned into SmaI and XhoI sites of pGL3-Basic plasmid (Promega). Deletion mutants of the rat AVP promoter were generated by

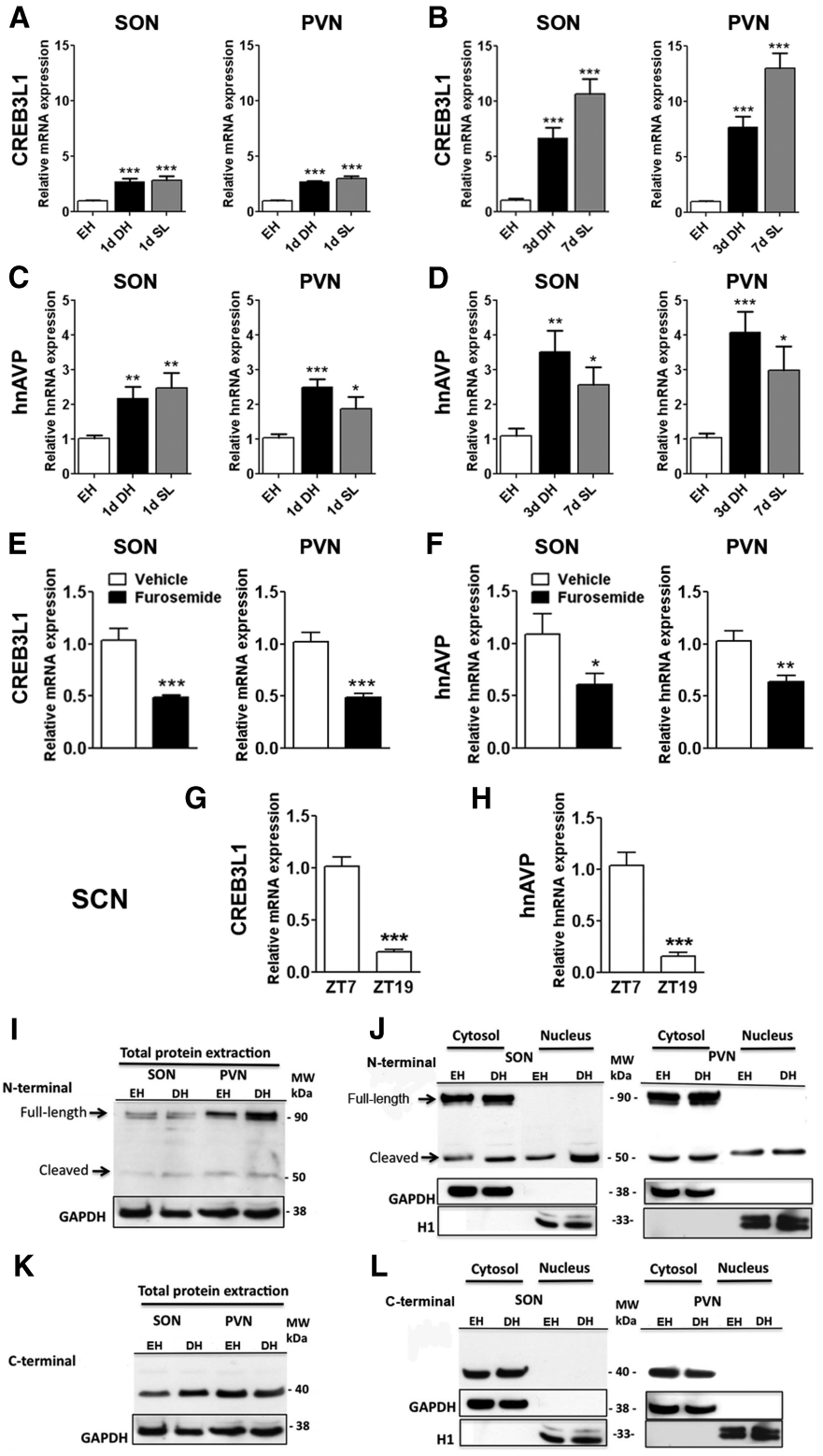

Figure 1. CREB3L1 and AVP expression in rat SONs and PVNs. The expression of CREB3L1 was examined in SONs and PVNs in hyperosmotic and hypo-osmotic conditions, and in SCNs in diurnal rhythm. ***A–H***, Relative mRNA expression of CREB3L1 and hnAVP was investigated by qPCR in SONs and PVNs of EH, DH (1 and 3 d), and SL (1 and 7 d) rats (***A–D***), SONs and PVNs of rats injected with 10 mg/kg furosemide at 24 h after injection (***E***, ***F***), and rat SCNs collected at ZT7 and ZT19 (***G***, ***H***). ***I–L***, CREB3L1 protein expression was investigated by Western blotting in both total and compartmentalized proteins (cytosol and nucleus) using antibodies raised against N-terminal (***I***, ***J***) and C-terminal (***K***, ***L***) epitopes. The proteins were extracted from SONs and PVNs ($n = 3$ per sample) of EH or 3 d DH rats. GAPDH and histone 1 (H1) were used as internal controls. Values are means ± SEM of $n = 6$ animals per group. $^{*}p < 0.05$, $^{**}p < 0.01$, $^{***}p \leq 0.001$. MW, molecular weight.

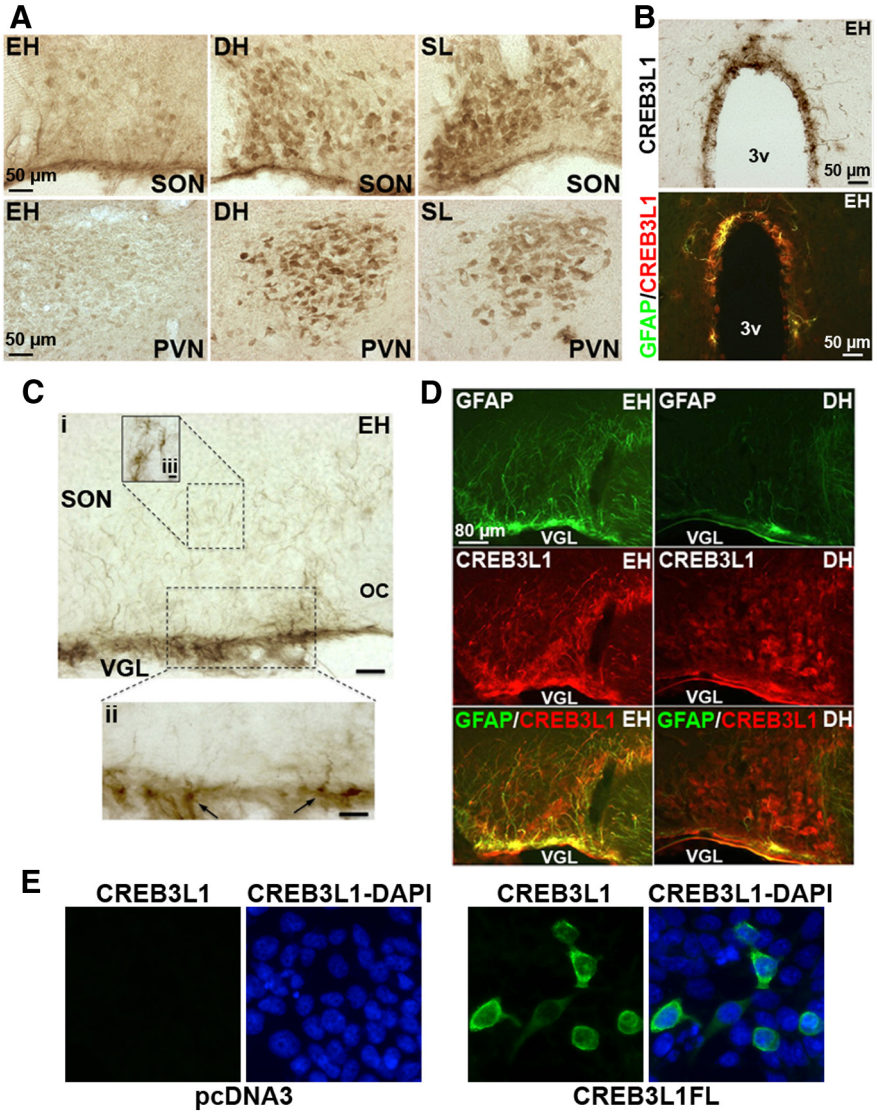

Figure 2. Localization of CREB3L1 expression in rat SONs and PVNs. CREB3L1 expression in SONs and PVNs was examined by immunostaining using an antibody against N-terminal CREB3L1. ***A***, Immunohistochemical staining of CREB3L1 in SONs and PVNs of EH, 3 d DH, and 7 d SL rats. ***B***, Immunohistochemical analysis of CREB3L1 and immunofluorescent colocalization of GFAP (green) and CREB3L1 (red) in glia cells surrounding the third ventricle of EH rats. ***C***, ***i–iii***, High-magnification images of CREB3L1 staining in SONs of EH rats (***i***) showed expression of CREB3L1 in glia cells in ventral glia lamina (***ii***) and the area of SONs (***iii***) in EH rats. ***D***, Colocalization of GFAP (astrocyte marker; green) and CREB3L1 (red) in SONs of EH and DH rats. ***E***, CREB3L1 immunofluorescence in HEK293T cells transfected with plasmid-expressing CREB3L1FL or pcDNA3. DAPI staining indicates nucleus. oc, Optic chiasm; VGL, ventral glia lamina; 3v, third ventricle. Scale bars: ***Ci***, 50 μm; ***Cii***, 25 μm; ***Ciii***, 10 μm.

overlap extension PCR. Primers 350_F and 350_R were designed to amplify 350 bp of the rat AVP promoter, and contained KpnI and XhoI restriction sites, respectively. These primers were used in combination with deletion-specific reverse and forward primers to amplify AVP promoter fragments using Phusion High-Fidelity DNA Polymerase (New England BioLabs). The PCR products from the initial PCRs were combined and used as a template for a subsequent PCR using primers 350_F and 350_R. The site-directed deletions (−55 bp, CRE1, CRE2, G-box, or AP2) and complete 350 bp fragment were ligated into the KpnI and XhoI sites of pGL3-Basic plasmid. Luciferase assays were performed in HEK293T cells according to the Promega Dual-Luciferase Reporter Assay System protocol. Luciferase activity was measured in triplicate using a Lumat LB 9507 Luminometer (Berthold Technologies). The following primers were used for site-directed deletions: 350_F 5′-CGG*GGTACC*AATGAGACCTGGGGACCCCT-3′ (KpnI); 350_R 5′-CCCG*CTCGAG*CCTGAGCGGGCTGGGCTGT-3′ (XhoI); CRE1 del_1R 5′-TCACTGGCCACCGTGGCCACCGCCACAGTGATT-3′; CRE1 del_2F 5′-CACGGTGGCCAGTGACAGCCT-3′; CRE2 del_1R 5′-AGCTGACAGGTCCCAGCAGTGATTC AGGCATCT-3′; CRE2 del_2F 5′-TGGG ACCTGTCAGCTGTGGG-3′; 55 bp del_1R 5′-CCACAGCTGACAGGTCCCAGGGTGGTG GAGGAGGGGAGCCA-3′; 55 bp del_2F 5′-TGGGACCTGTCAGCTGTGG-3′; ACGT del_1R 5′-TGATTCAGGCATCTGGGGACA CGGGCCTGTCAATGCAGAGGG-3′; ACGT del_2F 5′-GTGTCCCCAGATGCCTGAATCA-3′; G-box del_1R 5′-AGTGATTCAGGCAT CTGGGGCTGTCAATGCAGAGGGTGGT-3′; G-box del_2F 5′-CCCCAGATGCCTGAAT-CACT-3′; AP2 del_1R 5′-AGCTGTCAGCAGT-GATTCAGCACACGTGGGCCTGTCAATG-3′; and AP2 del_2F 5′-CTGAATCACTGCTGA CAGCT-3′.

Chromatin immunoprecipitation assay. The chromatin immunoprecipitation (ChIP) assay was performed on HEK293T cells following cotransfection with pGL3–1kb AVP promoter and CREB3L1CA by the calcium phosphate method. After 48 h, cells were harvested and 1×10^6 cells were diluted in 500 μl of PBS. For *in vivo* analyses of CREB3L1 binding, SONs were dissected from a 1 mm hypothalamic slice and immediately homogenized in 500 μl of PBS. ChIP assays were performed using 1 μg of a goat anti-CREB3L1 antibody (R&D Systems) using the LowCell ChIP kit protein G (kch-maglow-G16, Diagenode) following the manufacturer's protocol. DNA shearing was performed using Soniprep 150 sonicator (six rounds of 20 s on/20 s off at 2 μA). Normal goat IgG (Abcam) and anti-RNA polymerase II antibody (Millipore) were used as negative and positive controls, respectively. Isolated DNA samples were subjected to PCR and qPCR analysis using AVP promoter primers (5′-CACCACCCTCTGCATTGAC-3′ and 5′-GTCTGCAGGTGTTGGCTAGG-3′). PCRs were performed using TaqDNA polymerase (New England BioLabs).

Lentivirus production, purification, and titration. The cDNA clone encoding CREB3L1CA was cloned into lentiviral transfer vector pRRL.SIN.CPPT.CMV.IRES-GFP.WPRE. A lentiviral vector expressing GFP (pRRL.SIN-.CPPT.CMV.GFP.WPRE) was used as a control (Addgene). The transfer vectors were propagated in Stbl3-competent cells (Invitrogen) to reduce homologous recombination. All plasmid constructs were purified by Maxiprep using PureLink HiPure Plasmid Filter Maxiprep kit (Invitrogen). Viruses were generated by transient transfection of the transfer vector together with three separate packaging plasmids (pMDLg/pRRE, pRSV-Rev, PMD2.G; Addgene) into HEK293T cells by the calcium phosphate method, as previously described (Panyasrivanit et al., 2011). Culture supernatant containing lentivirus was collected at 48 and 72 h after transfection, cell debris was removed by centrifugation, and the supernatant was filtered through a 0.45 μm filter (catalog #430770, Corning). High-titer lentiviruses were produced by centrifugation at 6000 × *g* for 16 h (400 ml), followed by ultracentrifugation of the resuspended pellet (10 ml of PBS) for 1.5 h at 50,000 × *g*. The viral pellet was resuspended in 150 μl of prewarmed PBS and stored in 5 μl aliquots at −80°C. Viral titers were determined by counting GFP-positive cells at day 3 following infection of HEK293T cells.

Lentiviral vector gene transfer into SONs and PVNs. Rats were anesthetized by intraperitoneal administration of Domitor/ketamine and placed in a stereotaxic frame in the flat skull position. A 2 cm rostral–caudal

incision was made to expose the surface of the skull. Two 1 mm holes were drilled at coordinates 1.3 mm posterior to bregma and 1.8 mm lateral to midline for SON injection. A further two 1 mm holes were drilled at coordinates 1.8 mm posterior to bregma, and 0.4 mm lateral to midline for PVN injection. A 5 μl pulled glass pipette was positioned −8.8 mm (SON) or −7.4 mm (PVN) ventral to the surface of the brain, and 1 μl of lentiviral vector was delivered separately into four nuclei over 10 min. After surgery, animals were individually housed in standard laboratory cages for 2 weeks before being transferred to metabolic cages (TECHNIPLAST) to allow precise daily measurements of fluid intake, food intake, and urine output. Animals were weighed and allowed to acclimatize to the cage for 72 h. Fluid intake, food intake, and urine output were recorded for 7 d. Animals were killed by stunning and decapitation. Trunk blood was collected, and brains were snap frozen on dry ice and stored at −80°C. The posterior lobe of the pituitary gland was removed and placed in 500 μl of 0.1 M HCl, sonicated for 15 s, and incubated at 85°C for 20 min. Cellular debris was removed by centrifugation at 1000 × *g* for 1 h. Extracted plasma and pituitary AVP levels were determined by ELISA (ADI-900–017; Enzo Life Sciences). Osmolality was measured on 100 μl of plasma or urine by freezing point depression using a Roebling micro-osmometer (Camlab).

Statistical analysis. All data are expressed as the mean ± SEM. Statistical differences between qPCR experimental groups were evaluated using independent-sample unpaired Student's *t* tests. One-way ANOVA with Tukey's *post hoc* test were used to determine the differences between more than two groups with only a single influencing factor. Data in Figure 5*A* were log transformed before analysis due to unequal SDs within the dataset. $p < 0.05$ was considered significant.

Results

Profiling CREB3L1 mRNA and AVP hnRNA expression dynamics in rat hypothalamic nuclei in response to different physiological cues

We first investigated the time course of CREB3L1 mRNA expression in SON and PVN of euhydrated (EH), DH, and SL rats by qPCR. CREB3L1 mRNA expression was significantly higher in SONs and PVNs of 1 d DH rats (SON: 2.70 ± 0.30, $p = 2.92e^{-05}$; PVN: 2.70 ± 0.11, $p = 6.18e^{-09}$) and 1 d SL rats (SON: 2.85 ± 0.36, $p = 7.32e^{-05}$; PVN: 3.01 ± 0.23, $p = 5.66e^{-07}$) compared with EH rats (SON, 1.01 ± 0.05; PVN, 1.01 ± 0.06; Fig. 1*A*). Extending the duration of hyperosmotic stress to 3 d DH rats, and 7 d SL rats, further increased the magnitude of this response in both the SONs (EH: 1.05 ± 0.14; 3 d DH: 6.67 ± 0.94, $p = 1.52e^{-04}$; 7 d SL: 10.69 ± 1.33, $p = 2.93e^{-05}$) and PVNs (EH: 1.00 ± 0.03; 3 d DH: 7.69 ± 0.95, $p = 3.47e^{-05}$; 7 d SL: 13.02 ± 1.33, $p = 4.00e^{-06}$; Fig. 1*B*). In parallel, we observed an increase in AVP hnRNA expression in both SONs and PVNs of DH and SL rats, compared with EH animals (Fig. 1*C*: 1 d SONs: EH, 1.02 ± 0.09; DH, 2.17 ± 0.34, $p = 0.003$; SL, 2.47 ± 0.44, $p = 0.003$; 1 d PVNs: EH, 1.04 ± 0.11; DH, 2.48 ± 0.24, $p = 6.46e^{-05}$; SL, 1.86 ± 0.35, $p = 0.024$; Fig. 1*D*: SONs: EH, 1.09 ± 0.23; 3 d DH, 3.50 ± 0.61, $p = 0.004$; 7 d SL, 2.56 ± 0.50, $p = 0.024$; PVN EH, 1.04 ± 0.13; 3 d DH, 4.07 ± 0.60, $p = 5.88e^{-04}$; 7 d SL, 2.98 ± 0.68, $p = 0.019$), which is indirectly indicative of increased AVP gene transcription (Yue et al., 2006a). In contrast, sodium depletion induced by 24 h of furosemide treatment significantly reduced CREB3L1 mRNA (SON: 0.48 ± 0.03, $p = 4.56e^{-04}$; PVN: 0.49 ± 0.04, $p = 3.66e^{-04}$; Fig. 1*E*) and hnRNA of vasopressin (hnAVP) expression (SON: 0.61 ± 0.11, $p = 0.049$; PVN: 0.64 ± 0.06, $p = 0.007$; Fig. 1*F*) in both SONs and PVNs compared with vehicle time-matched controls (SONs: CREB3L1, 1.03 ± 0.12; hnAVP, 1.08 ± 0.20; PVNs: CREB3L1, 1.02 ± 0.09; hnAVP, 1.03 ± 0.10). In another well defined vasopressin-expressing

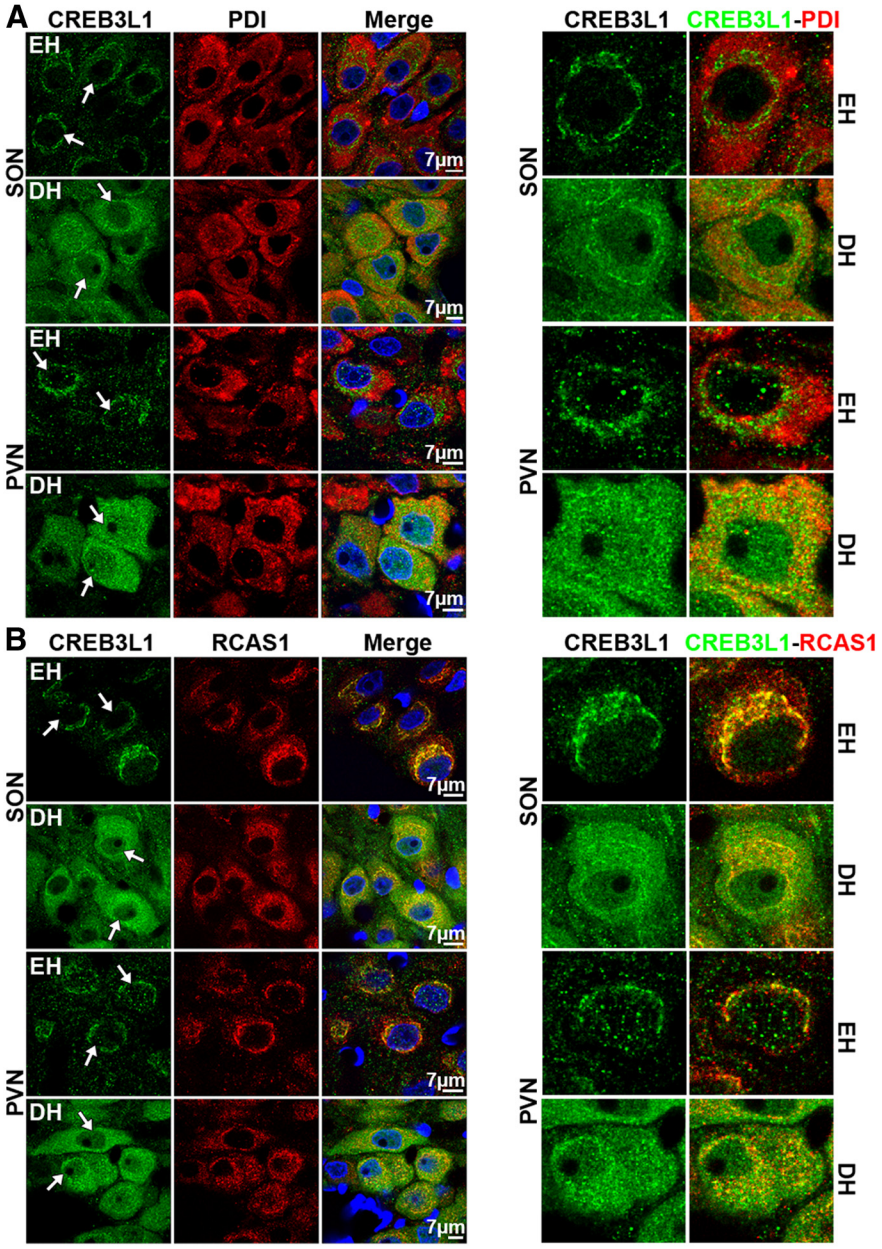

Figure 3. Shifting cellular localization of CREB3L1 expression in SONs and PVNs with osmotic challenge. Immunofluorescent staining of CREB3L1 (green) with PDI (ER marker; red; ***A***) or RCAS1 (Golgi marker; red; ***B***) in SONs and PVNs of EH and 3 d DH rats. Single-cell pictures are shown in the right panel. Cell nuclei were stained with DAPI (blue). The images were obtained using confocal microscope. Arrows indicate nuclei of MCNs.

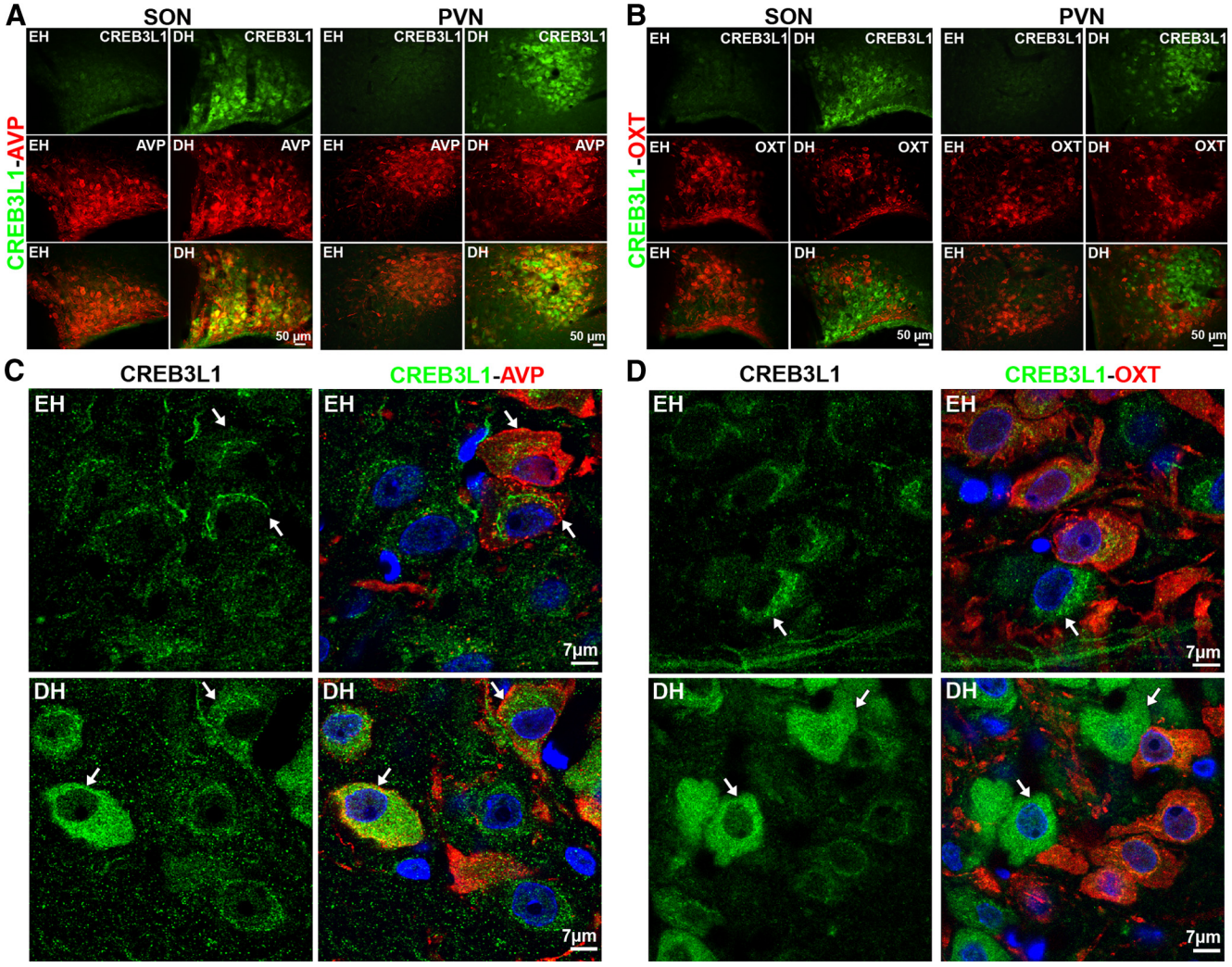

Figure 4. CREB3L1 is activated predominantly in vasopressinergic neurons in response of hyperosmotic stress. ***A***, ***B***, Immunofluorescent colocalization of CREB3L1 (green) with either AVP (red; ***A***) or OXT (red; ***B***) in SONs and PVNs of EH and 3 d DH rats. ***C***, ***D***, Confocal images showing colocalization of CREB3L1 (green) with AVP (red; ***C***) or OXT (red; ***D***) in MCNs of EH and 3 d DH rats. Cell nuclei stained with DAPI (blue). Arrows indicate AVP-expressing MCNs.

brain nucleus, the SCN, the level of CREB3L1 mRNA expression (ZT7, 1.02 ± 0.09; ZT19, 0.19 ± 0.02; $p = 4.01e^{-06}$; Fig. 1*G*) correlated with the circadian rhythm of hnAVP expression (ZT7, 1.04 ± 0.13; ZT19, 0.15 ± 0.04; $p = 6.62e^{-05}$; Fig. 1*H*; Uhl and Reppert, 1986; Maruyama et al., 2010).

Expression of CREB3L1 protein in rat hypothalamus

The expression of different processed forms of the CREB3L1 protein was then investigated by Western blotting using antibodies raised against either N- or C-terminal epitopes of CREB3L1. Using an antibody recognizing the N-terminal transcriptional activation domain (NT-CREB3L1), two bands migrating at ~90 kDa (full-length; Chihara et al., 2009) and 50 kDa (cleaved N-terminal domain; Chihara et al., 2009) were identified in total protein extracts from SONs and PVNs of EH and DH rats (Fig. 1*I*). Separation of EH and DH SONs and PVNs into cytosolic and nuclear protein fractions revealed both full-length 90 kDa and cleaved 50 kDa proteins in the cytosol, but only the 50 kDa band was observed in nuclear fractions (Fig. 1*J*). Using the antibody recognizing the C-terminal portion of CREB3L1, a single band migrating at ~40 kDa was observed in immunoblots of total SON and PVN protein (Fig. 1*K*). This band was detected only in cytoplasmic protein extracts, not in the nuclear protein extracts of the SONs and PVNs, and likely represents a C-terminal cleaved fragment of CREB3L1 (Fig. 1*L*). Although the intensity of the 50 kDa NT-CREB3L1 band appeared higher in SON nuclear fractions of DH compared with EH rats (Fig. 1*J*), implying activation of CREB3L1 during hyperosmotic stress, the lack of a robust overall increase in protein abundance contrasted with the dramatic increase in transcript levels.

Shifting cellular localization of CREB3L1 expression in SONs and PVNs with osmotic challenge

Immunohistochemical localization was then performed to examine which cell populations express CREB3L1 in the SONs and PVNs of EH and DH rats (Fig. 2*A*). In EH rats, robust expression was seen in the glia cells lining the third ventricle (Fig. 2*B*) and in astrocytes of the ventral glia limitans (Fig. 2*C*). In contrast, only weak staining was observed in MCNs of the SONs and PVNs (Fig. 2*A*). However, a striking increase of CREB3L1 staining in neuronal cell bodies was clearly evident following 3 d of DH and 7 d of SL, compared with controls (Fig. 2*A*). The increase in neuronal expression coincided with decreased staining of glial processes with an astrocyte marker,

GFAP, in SONs of DH rats compared with EH rats (Fig. 2*D*), indicating glial retraction in response to hyperosmotic stress, as previously reported (Salm and Hawrylak, 2004). The specificity of the N-terminal CREB3L1 antibody was assessed in HEK293T cells transfected with rat CREB3L1FL (Fig. 2*E*).

Further, changes in the subcellular distribution of CREB3L1 in MCNs were seen following 3 d of DH, consistent with functional activation. Confocal images showed that, in EH rats, CREB3L1 staining was predominantly confined to perinuclear areas of MCNs, whereas following DH, staining was observed throughout the cell cytoplasm (Fig. 3*A*,*B*). A degree of CREB3L1 colocalization with PDI (Fig. 3*A*, ER marker) and a strong colocalization with receptor binding cancer antigen expressed on SiSo cells (RCAS1; Fig. 3*B*, Golgi marker) in SONs and PVNs of EH rats was observed. An increase in CREB3L1 colocalization with the ER marker in MCNs was observed in DH compared with EH rats. CREB3L1 immunostaining was also observed in the nuclei of MCNs in 3 d DH rats, in contrast to its absence from this structure in EH rats (Fig. 3*A*,*B*, arrows).

To examine the identity of SON and PVN neuronal cell populations expressing CREB3L1, double-immunofluorescent staining of CREB3L1 with AVP NP-I (Fig. 4*A*) or OXT NP-II (Fig. 4*B*) was performed. In control EH rats, weak staining of CREB3L1 was observed in AVP and OXT MCNs of the SON and PVN (Fig. 4*A*,*B*). A high degree of colocalization of CREB3L1 and AVP neurons was observed in SONs and PVNs of 3 d DH rats (Fig. 4*A*), with weaker staining of CREB3L1 in OXT neurons (Fig. 4*B*). Confocal images showed that the changes in subcellular localization of CREB3L1 following 3 d DH were confined to AVP neurons (Fig. 4*C*). Thus, in response to hyperosmotic stress, CREB3L1 expression increases predominantly in AVP, not OXT MCNs (Fig. 4*D*).

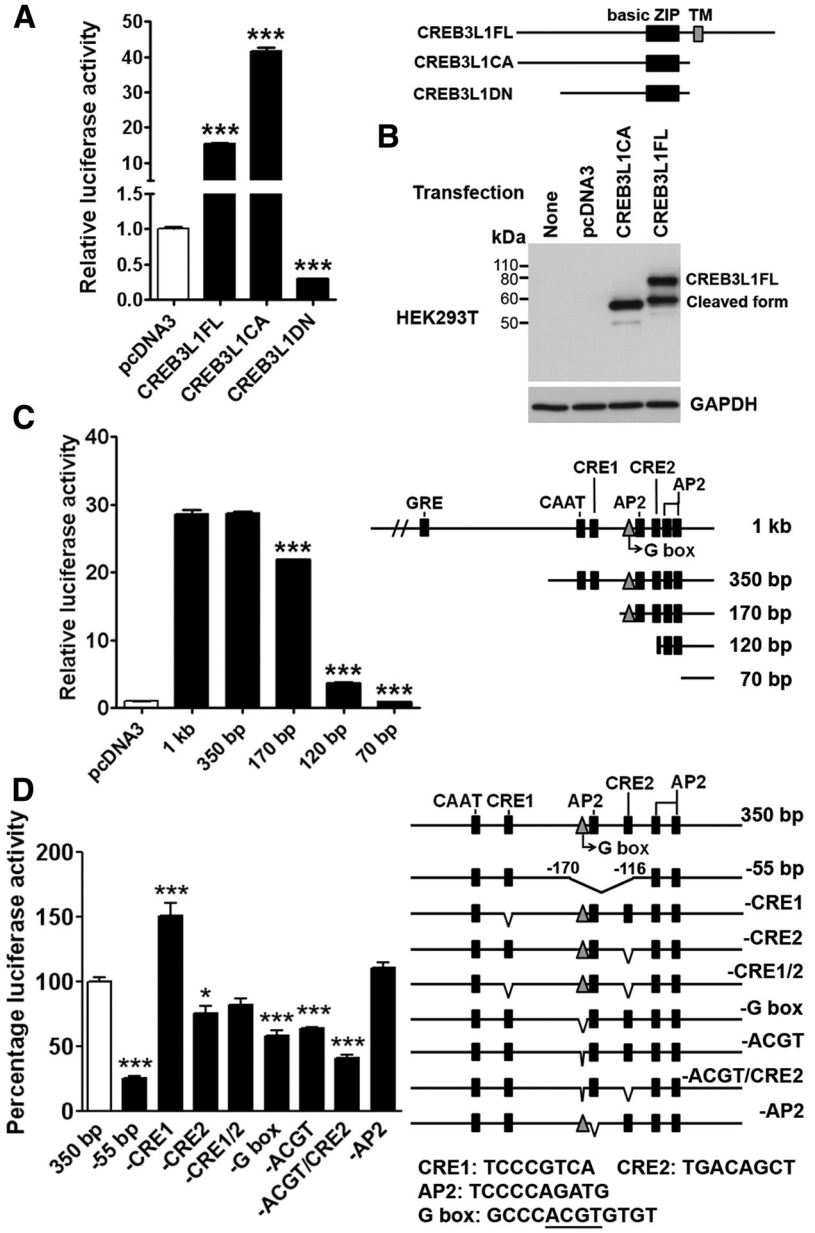

Figure 5. CREB3L1 acts on AVP promoter. ***A***, Luciferase assays were performed in HEK293T cells transfected with plasmid containing 1 kb rat AVP promoter together with plasmids expressing CREB3L1FL, CREB3L1CA, or CREB3L1DN. ***B***, Western blot of CREB3L1 in HEK293T cells transfected with pcDNA3, CREB3L1CA, and CREB3L1FL. ***C***, Luciferase assays using plasmids containing 1 kb, and 350, 170, 120, or 70 bp deletion constructs of rat AVP promoter–luciferase reporter together with plasmid expressing CREB3L1CA. ***D***, Luciferase assay using site-directed deletion constructs of the rat AVP promoter. The experiments were performed in at least three independent replicates. Error bars indicate mean ± SEM. $^{*}p < 0.05$, $^{***}p \leq 0.001$. Basic ZIP, Basic leucine zipper domain; TM, transmembrane domain; GRE, glucocorticoid-responsive element (−622 to −608 bp); CAAT, CAAT box (−246 to −243 bp); CRE1, −228 to −221 bp; CRE2, −123 to −116 bp); AP2, −146 to −137 bp, −95 to −86 bp and −84 to −75 bp; G-box (−157 to −146 bp); ACGT, −153 to −150 bp.

CREB3L1 regulates AVP transcription by binding to the AVP promoter

The expression of CREB3L1 in vasopressinergic neurons, coupled with the strong correlation with AVP hnRNA levels in a number of models, suggested that CREB3L1 may regulate AVP gene expression. To investigate CREB3L1 actions on the AVP promoter *in vitro*, luciferase assays were performed in HEK293T cells. Expression of CREB3L1FL and CREB3L1CA significantly increased luciferase activity by 15.49 ± 0.24-fold ($p < 0.001$) and 41.63 ± 1.11-fold ($p < 0.001$), respectively, compared with controls (pcDNA3, 1 ± 0.03; Fig. 5*A*). In contrast, the expression of CREB3L1DN reduced luciferase activity (0.30 ± 2.11e^{-04}, $p < 0.001$; Fig. 5*A*). Immunoblot analysis of CREB3L1FL expression in HEK293T cells detected two bands, indicating CREB3L1 processing (Fig. 5*B*).

To identify CREB3L1 interaction sites in the AVP promoter, luciferase assays were performed on deletion constructs (1 kb, and 350, 170, 120, or 70 bp) of the rat AVP promoter (Fig. 5*C*, diagram). Truncating the AVP promoter from 1 kb to 350 bp had no effect on CREB3L1CA-mediated luciferase activity (1 kb, 28.61 ± 0.63; 350 bp, 28.66 ± 0.31; $p = 1.000$). A small, but significant, decrease of luciferase activity was observed with the 170 bp AVP promoter construct (21.86 ± 0.10, $p < 0.001$) com-

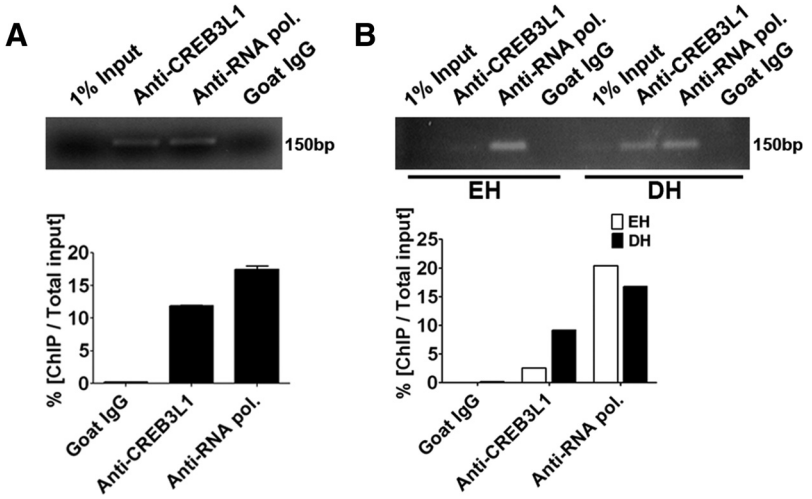

Figure 6. CREB3L1 regulates AVP transcription by binding to the AVP promoter. ChIP assays were performed using antibody against N-terminal CREB3L1. ***A***, HEK293T cells were transfected with plasmid containing 1 kb rat AVP promoter and plasmid expressing CREB3L1CA ($n = 3$). ***B***, ChIP assay was performed using pooled ($n = 3$) SON samples from EH and 3 d DH rats. Normal goat IgG and anti-RNA polymerase II antibody were used as negative and positive controls, respectively. Percentage of ChIP/total input was calculated. PCR products from ChIP assay were verified by gel electrophoresis, showing 150 bp PCR products. Error bars indicate mean ± SEM. RNA pol., RNA polymerase II.

pared with the 1 kb promoter. Luciferase activity dropped sharply with the AVP 120 bp promoter construct (3.68 ± 0.16, $p < 0.001$), with levels reaching basal when only 70 bp of the AVP promoter remained (0.95 ± 0.01, $p < 0.001$; Fig. 5*C*). Thus, CREB3L1 actions on the AVP promoter are mediated by sequences located between −170 and −120 bp. This crucial region contains CRE-like, AP2, and G-box elements, all of which are potential binding motifs for CREB3L1 (Pardy et al., 1992; Iwasaki et al., 1997; Jolma et al., 2013). Accordingly, a series of site-specific deletion mutants of the 350 bp rat AVP promoter were generated (Fig. 5*D*, diagram). First, to confirm and strengthen earlier findings, a 55 bp fragment of the AVP promoter was deleted, including the full CRE2 site. This produced a profound drop in luciferase activity (25.28 ± 2.31%, $p < 0.001$, where 350 bp is 100%; Fig. 5*D*), consistent with earlier findings with the AVP promoter −120 bp construct (Fig. 5*C*). Deletion of CRE1 and CRE2 sites significantly increased (150.80 ± 10.29%, $p < 0.001$) and decreased (75.93 ± 5.62%, $p = 0.042$) luciferase activity, respectively, while deletion of both CRE sites showed no change in luciferase activity (82.47 ± 4.96%, $p = 0.285$; Fig. 5*D*). Deletion of the G-box (58.58 ± 3.91%, $p < 0.001$) and the ACGT motif (63.77 ± 0.91%, $p = 0.001$) also decreased luciferase activity (Fig. 5*D*). A combination of CRE2 and ACGT deletions produced the most significant drop (40.75 ± 2.76%, $p < 0.001$) in luciferase activity, emphasizing the importance of these binding sites (Fig. 5*D*). No significant change in luciferase activity resulted from deletion of the AP2 site (110.72 ± 4.31%, $p = 0.846$).

To demonstrate direct binding of CREB3L1 to the AVP promoter, ChIP was performed. In HEK293T cells, the CREB3L1-binding DNA fragments were identified by PCR and qPCR using specific rat AVP promoter primers. The correctly sized band (150 bp) was observed in CREB3L1 immunoprecipitated DNA (Fig. 6*A*), suggesting binding of CREB3L1 to the AVP promoter. No band was observed in IgG-negative controls, while the success of the ChIP protocol was confirmed by a band in the RNA polymerase II-positive control. To demonstrate *in vivo* binding of CREB3L1 to the AVP promoter, ChIP was performed on SON chromatin extracts from EH and DH rats (Fig. 6*B*). Again, PCR confirmed the presence of AVP promoter in CREB3L1 immunoprecipitates from SONs of EH and DH rats. An increase in band intensity in ChIP from DH rat SON samples was validated by qPCR, indicating increased binding to the AVP promoter during DH.

CREB3L1 positively regulates expression of AVP in rat SON and PVN *in vivo*

We overexpressed CREB3L1CA in rat SONs and PVNs by lentiviral vector delivery. Quantification by qPCR confirmed the successful overexpression in both SONs (GFP, 1.01 ± 0.05; CREB3L1CA, 1.23 ± 0.09; $p = 0.038$; Fig. 7*A*) and PVNs (GFP, 1.01 ± 0.05; CREB3L1CA, 1.38 ± 0.09; $p = 0.004$; Fig. 7*A*). An increase in AVP mRNA was observed in PVNs (GFP, 1.03 ± 0.09; CREB3L1CA, 1.43 ± 0.08; $p = 0.003$; Fig. 7*B*), but not SONs (GFP, 1.02 ± 0.07; CREB3L1CA, 1.11 ± 0.13; $p = 0.522$; Fig. 7*B*), while higher hnAVP was observed in both SONs (GFP, 1.03 ± 0.08; CREB3L1CA, 1.50 ± 0.12; $p = 0.004$; Fig. 7*C*) and PVNs (GFP, 1.03 ± 0.09; CREB3L1CA, 1.73 ± 0.16; $p = 0.002$; Fig. 7*C*). Furthermore, pituitary AVP peptide content was higher in CREB3L1CA rats (545.32 ± 13.56 ng/gland, $p = 0.003$) compared with GFP controls (453.5 ± 8.47 ng/gland; Fig. 7*D*). No significant difference in plasma AVP between CREB3L1CA-expressing rats (2.93 ± 1.38 pg/ml, $p = 0.442$) and GFP-expressing rats (1.54 ± 0.37 pg/ml) was observed (Fig. 7*E*), and osmotic homeostasis was unaffected (Fig. 7*F–I*).

Discussion

Using Affymetrix oligonucleotide microarrays, we compiled transcriptome catalogs that represent comprehensive descriptions of the mRNA populations in the SONs and PVNs, and we identified transcripts that change in their expression in response to hyperosmotic stress (Hindmarch et al., 2006). We predicted that some of these transcriptome changes might be mediated by altered transcription factor activity, so we proceeded to examine our data to identify transcription factors regulated by hyperosmotic stress in both rat and mouse (Qiu et al., 2007; Stewart et al., 2011). These data brought the transcription factor CREB3L1 to our attention.

We have previously reported upregulated CREB3L1 expression in the rat hypothalamus following 3 d DH (Qiu et al., 2007), but its functional role remained elusive. In the current study, we have validated CREB3L1 transcriptome-derived data by qPCR over the time course of two osmotic stimuli, DH and SL. The consistent increases in CREB3L1 mRNA expression, and the parallel changes in AVP hnRNA, merited further investigation into CREB3L1 at the protein level.

CREB3L1 is one of five members of the CREB3 bZIP transcription factor subfamily (Kondo et al., 2011). All CREB3 transcription factors are structurally similar to activating transcription factor 6, a classical ER stress transducer (Murakami et al., 2006; Asada et al., 2011). Inactive CREB3L1 is anchored into the ER membrane (Omori et al., 2002). In response to stimuli, CREB3L1 is transported

from ER to the Golgi complex, where it is activated by regulated intramembrane proteolysis. The liberated N-terminal active fragment then translocates to the nucleus (Murakami et al., 2006), where it activates the transcription of target genes defined by specific *cis*-acting regulatory promoter sequences (Kondo et al., 2005; Murakami et al., 2009). As expected, Western blotting revealed full-length and the C-terminal cleaved forms of CREB3L1 in cytosolic SON and PVN protein extracts, but not in nuclear extracts, whereas the N-terminal active fragment was found in both cytosol and nucleus (Fig. 1*J*,*L*). However, in contrast to the robust changes seen in CREB3L1 mRNA levels (Fig. 1*A*,*B*), we were surprised to see only modest increases in protein levels. Immunohistochemistry provided an explanation for this paradox. In EH rats, robust constitutive expression is seen in SON and PVN glia cells, with only low-level expression of CREB3L1 seen in both OXT and AVP MCNs. It is only after DH or SL that the increase in CREB3L1 expression results in accumulation of CREB3L1, predominantly in AVP neurons (Figs. 2, 4).

Immunocytochemical investigation of the subcellular localization of CREB3L1 in SONs and PVNs of EH and DH rats provided further evidence of functional activation following an osmotic stimulus. Previous *in vitro* studies on unstimulated C6 glioma cells showed CREB3L1 to be located in perinuclear ER structures (Kondo et al., 2005). However, here we show that in EH rat MCNs, CREB3L1 is poorly colocalized with the ER marker PDI, whereas a stronger colocalization was observed following DH, perhaps due to increased synthesis and subsequent ER accumulation. The strong colocalization of CREB3L1 with Golgi marker RCAS1 in MCNs of both EH and DH rats indicates that CREB3L1 is likely cleaved and activated in the Golgi apparatus, as previously reported (Murakami et al., 2006). The mechanism of CREB3L1 activation in MCNs remains unknown. Interestingly, only after DH did we observe marked CREB3L1 localization in MCN nuclei (Fig. 3). Thus, the cytosolic accumulation of CREB3L1 implies that, in MCNs, gating mechanisms regulate the entry of NT-CREB3L1 into the nucleus.

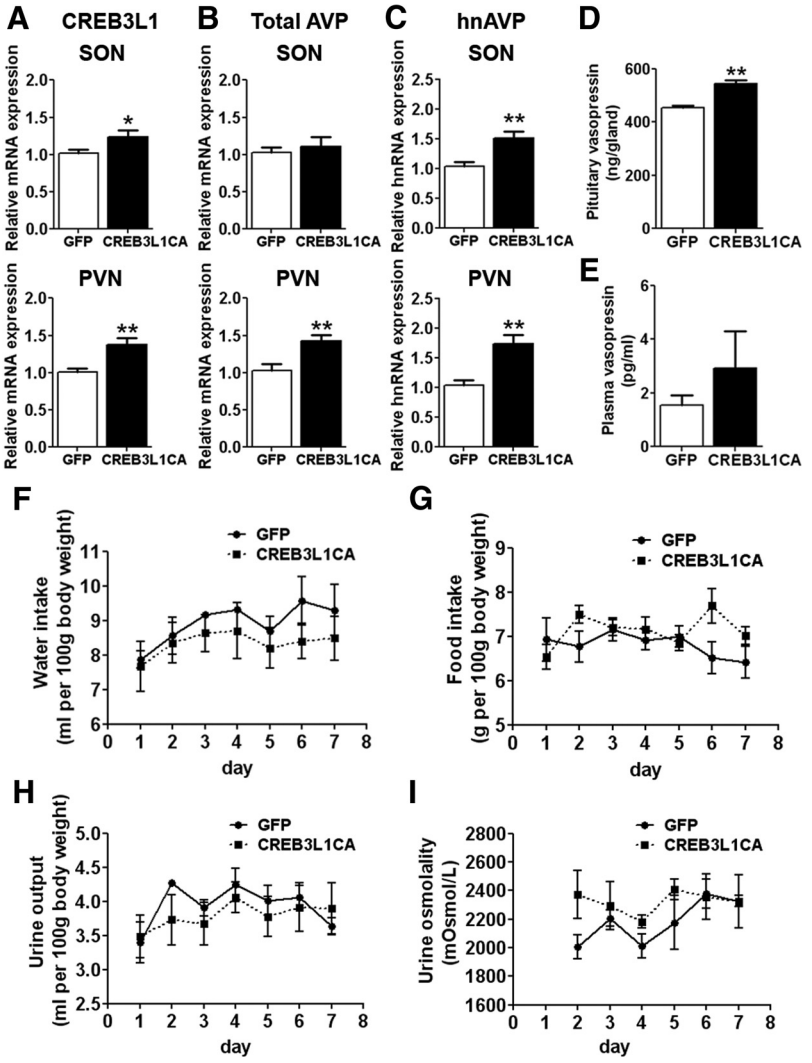

Figure 7. CREB3L1 regulates expression of the AVP gene in rat SONs and PVNs. Rats were bilaterally injected into SONs and PVNs with lentiviral vectors expressing either CREB3L1CA or GFP. ***A–C***, The relative expression of CREB3L1 mRNA (***A***), total AVP mRNA (***B***), and AVP hnRNA (***C***) in SONs and PVNs was examined by qPCR (GFP, $n = 10$ for SONs and $n = 9$ for PVNs; CREB3L1CA, $n = 7$ for SONs and $n = 13$ for PVNs). ***D***, ***E***, Pituitary AVP (***D***) and plasma AVP (***E***) levels were examined by ELISA. ***F–I***, Two weeks after injection, the rats were placed in metabolic cages for 7 d where water intake (***F***), food intake (***G***), urine output (***H***), and urine osmolality (***I***) were recorded. For ***D–I***, only data from rats with successful overexpression of CREB3L1CA in four nuclei were included (GFP $n = 3$, CREB3L1CA $n = 4$). Error bar indicated mean ± SEM. $^{*}p < 0.05$, $^{**}p < 0.01$.

As increased CREB3L1 expression was observed predominantly in vasopressinergic MCNs following DH, we thus investigated the relationship between AVP and CREB3L1 expression in other paradigms. First, we looked at the hypo-osmotic challenge of furosemide-induced sodium depletion (Ray et al., 1991), where lower AVP hnRNA expression coincided with a significant fall in CREB3L1 mRNA expression in SONs and PVNs. CREB3L1 expression was also investigated in the SCN, where both AVP mRNA and hnRNA exhibit robust circadian expression profiles (Uhl and Reppert, 1986; Maruyama et al., 2010). In parallel with AVP hnRNA expression, we saw higher levels of CREB3L1 mRNA expression at ZT7 compared with ZT19. These findings lend support to the concept that CREB3L1 has the potential to regulate AVP transcription.

To test this notion, we asked whether CREB3L1 could support the expression of AVP gene promoter luciferase reporter constructs in HEK293T cells. Using a series of promoter–deletion constructs, the region between −170 and −120 bp was identified as important for CREB3L1 activation of the AVP promoter. This region contains a CRE-like sequence (CRE2), an AP2 site, and an E box enhancer (Pardy et al., 1992; Jin et al., 1999). However, deletion of the CRE2 resulted in only a 25% decrease in luciferase activity, opening the search for additional CREB3L1 binding sites within this 50 bp sequence. A number of sequences have been identified previously as CREB3L1 regulatory DNA binding sites, including ER stress response element (ERSE), unfolded protein response element and CRE-like sequences (Kondo et al., 2005; Murakami et al., 2009; Denard et al., 2011; Saito et al., 2012). Further, Jolma et al. (2013) recently performed a comprehensive

computer analysis of DNA binding sites of human CREB3L1. This study identified a 12 nucleotide CREB3L1 binding site (G-box) that was also found to be represented in rat, mouse, and human AVP promoters (GCCCACGTGTGT). The G-box flanks the previously identified E-box enhancer element (CACGTG), where CLOCK and BMAL1 bind to generate the circadian regulation of AVP transcription in the SCN (Jin et al., 1999). Here, we validated the CREB3L1 computational analysis by showing decreased luciferase activity following deletion of the G-box in rat AVP promoter. The 60% reduction in luciferase activity following deletion of ACGT of the G-box, together with CRE2, confirmed the importance of these sites for CREB3L1 actions on the AVP promoter. Moreover, Kondo et al. (2005) showed that two regulatory sequences (CRE and ERSE) are involved in CREB3L1 regulation of binding Ig protein gene transcription during ER stress. Interestingly part of the ERSE site (CCAAT-N9-*CCACG*) has sequence overlap with the G-box, lending support to the importance of the CRE site and the G-box element for CREB3L1 to function as an AVP gene transcription factor.

We then showed using ChIP that the transcriptional regulation of the AVP promoter by CREB3L1 was through direct binding, not only *in vitro*, but also *in vivo*, in the SON, with binding increasing with DH. We propose that this occurs, in part, through binding to G-box and CRE2 sites as identified here by luciferase assays. To further confirm that CREB3L1 regulates AVP transcription *in vivo*, a lentiviral vector expressing CREB3L1CA was injected bilaterally into both the SON and PVN. This resulted in increased expression of hnAVP in rat SONs and PVNs, strongly supporting the hypothesis that CREB3L1 is a direct positive regulator of AVP transcription. The increased AVP hnRNA expression resulted in an increase in the AVP content of the posterior pituitary, but no change in plasma AVP concentration, and no changes in a number of hemodynamic parameters. Thus, we suggest that increased AVP gene transcription leads to an increase in AVP mRNA, which is in turn translated, resulting in an accumulation of AVP peptide in the posterior pituitary. In the absence of an osmotic cue, this increased posterior pituitary AVP is not secreted.

Interestingly, *in vivo* deletion studies of the rat AVP promoter found that the region between −116 and −288 bp is important for cell-specific expression of AVP in MCNs (Ponzio et al., 2012). This region includes residues −120 to −170 bp and is consistent with the suggestion that CREB3L1 could play a part in MCN-specific expression of AVP. Failure to observe activation of CREB3L1 in OXT neurons following hyperosmotic stress implies that CREB3L1 in AVP and OXT MCNs is activated through separate pathways. Further investigation of CREB3L1 in additional experimental models is important to address functions in OXT MCNs. Furthermore, Ponzio et al. (2012) identified three upstream AVP transcriptional regulatory domains, one of which is located within the 1 kb fragment (−543 to −288 bp) of the rat AVP promoter in the present study, where no change in promoter activity was observed *in vitro*. This represents a limitation of performing the promoter studies in HEK293T cells.

In summary, our results showed that CREB3L1 is expressed in vasopressinergic neurons of the SON and PVN with markedly different cellular and subcellular locations in EH and DH animals. Within the rat AVP promoter, there are at least two CREB3L1 sites that we propose are important for direct binding and subsequent activation of AVP transcription. The ability to influence hnAVP transcripts *in vivo* by lentiviral gene transfer greatly strengthens our hypothesis that CREB3L1 is a major player in what is certainly a very complex and almost certainly highly redundant AVP gene transcriptional regulatory network. Indeed, preliminary experiments in which CREB3L1 activity was reduced *in vivo* by lentivirus-mediated delivery of CREB3L1DN revealed no change in AVP expression due to compensatory increases in the expression of mRNAs encoding other key transcription factors.

References

Adan RA, Burbach JP (1992) Regulation of vasopressin and oxytocin gene expression by estrogen and thyroid hormone. Prog Brain Res 92:127–136. CrossRef Medline

Antunes-Rodrigues J, de Castro M, Elias LL, Valença MM, McCann SM (2004) Neuroendocrine control of body fluid metabolism. Physiol Rev 84:169–208. CrossRef Medline

Asada R, Kanemoto S, Kondo S, Saito A, Imaizumi K (2011) The signalling from endoplasmic reticulum-resident bZIP transcription factors involved in diverse cellular physiology. J Biochem 149:507–518. CrossRef Medline

Ben-Barak Y, Russell JT, Whitnall MH, Ozato K, Gainer H (1985) Neurophysin in the hypothalamo-neurohypophysial system. I. Production and characterization of monoclonal antibodies. J Neurosci 5:81–97. Medline

Boone M, Deen PM (2008) Physiology and pathophysiology of the vasopressin-regulated renal water reabsorption. Pflugers Arch 456:1005–1024. CrossRef Medline

Bourque CW (2008) Central mechanisms of osmosensation and systemic osmoregulation. Nat Rev Neurosci 9:519–531. CrossRef Medline

Bradford MM (1976) A rapid and sensitive method for the quantitation of microgram quantities of protein utilizing the principle of protein-dye binding. Anal Biochem 72:248–254. CrossRef Medline

Carter DA, Murphy D (1989) Cyclic nucleotide dynamics in the rat hypothalamus during osmotic stimulation: in vivo and in vitro studies. Brain Res 487:350–356. CrossRef Medline

Carter DA, Murphy D (1990) Regulation of c-fos and c-jun expression in the rat supraoptic nucleus. Cell Mol Neurobiol 10:435–445. CrossRef Medline

Ceding P, Schilling K, Schmale H (1990) Vasopressin expression in cultured neurons is stimulated by cyclic AMP. J Neuroendocrinol 2:859–865. CrossRef Medline

Chihara K, Saito A, Murakami T, Hino S, Aoki Y, Sekiya H, Aikawa Y, Wanaka A, Imaizumi K (2009) Increased vulnerability of hippocampal pyramidal neurons to the toxicity of kainic acid in OASIS-deficient mice. J Neurochem 110:956–965. CrossRef Medline

Denard B, Seemann J, Chen Q, Gay A, Huang H, Chen Y, Ye J (2011) The membrane-bound transcription factor CREB3L1 is activated in response to virus infection to inhibit proliferation of virus-infected cells. Cell Host Microbe 10:65–74. CrossRef Medline

Hindmarch C, Yao S, Beighton G, Paton J, Murphy D (2006) A comprehensive description of the transcriptome of the hypothalamoneurohypophyseal system in euhydrated and dehydrated rats. Proc Natl Acad Sci U S A 103:1609–1614. CrossRef Medline

Honma Y, Kanazawa K, Mori T, Tanno Y, Tojo M, Kiyosawa H, Takeda J, Nikaido T, Tsukamoto T, Yokoya S, Wanaka A (1999) Identification of a novel gene, OASIS, which encodes for a putative CREB/ATF family transcription factor in the long-term cultured astrocytes and gliotic tissue. Brain Res Mol Brain Res 69:93–103. CrossRef Medline

Iwasaki Y, Oiso Y, Saito H, Majzoub JA (1997) Positive and negative regulation of the rat vasopressin gene promoter. Endocrinology 138:5266–5274. CrossRef Medline

Jin X, Shearman LP, Weaver DR, Zylka MJ, de Vries GJ, Reppert SM (1999) A molecular mechanism regulating rhythmic output from the suprachiasmatic circadian clock. Cell 96:57–68. CrossRef Medline

Jolma A, Yan J, Whitington T, Toivonen J, Nitta KR, Rastas P, Morgunova E, Enge M, Taipale M, Wei G, Palin K, Vaquerizas JM, Vincentelli R, Luscombe NM, Hughes TR, Lemaire P, Ukkonen E, Kivioja T, Taipale J (2013) DNA-binding specificities of human transcription factors. Cell 152:327–339. CrossRef Medline

Kondo S, Murakami T, Tatsumi K, Ogata M, Kanemoto S, Otori K, Iseki K, Wanaka A, Imaizumi K (2005) OASIS, a CREB/ATF-family member, modulates UPR signalling in astrocytes. Nat Cell Biol 7:186–194. CrossRef Medline

Kondo S, Saito A, Asada R, Kanemoto S, Imaizumi K (2011) Physiological unfolded protein response regulated by OASIS family members, trans-

membrane bZIP transcription factors. IUBMB Life 63:233–239. CrossRef Medline

Livak KJ, Schmittgen TD (2001) Analysis of relative gene expression data using real-time quantitative PCR and the 2(-delta delta C(T)) method. Methods 25:402–408. CrossRef Medline

Lubelski D, Ponzio TA, Gainer H (2012) Effects of A-CREB, a dominant negative inhibitor of CREB, on the expression of c-fos and other immediate early genes in the rat SON during hyperosmotic stimulation in vivo. Brain Res 1429:18–28. CrossRef Medline

Luckman SM, Dye S, Cox HJ (1996) Induction of members of the Fos/Jun family of immediate-early genes in identified hypothalamic neurons: in vivo evidence for differential regulation. Neuroscience 73:473–485. CrossRef Medline

Maruyama T, Ohbuchi T, Fujihara H, Shibata M, Mori K, Murphy D, Dayanithi G, Ueta Y (2010) Diurnal changes of arginine vasopressin-enhanced green fluorescent protein fusion transgene expression in the rat suprachiasmatic nucleus. Peptides 31:2089–2093. CrossRef Medline

McKinley MJ, McAllen RM, Davern P, Giles ME, Penschow J, Sunn N, Uschakov A, Oldfield BJ (2003) The sensory circumventricular organs of the mammalian brain. Adv Anat Embryol Cell Biol 172:III-XII, 1–122, back cover. Medline

Miselis RR (1981) The efferent projections of the subfornical organ of the rat: a circumventricular organ within a neural network subserving water balance. Brain Res 230:1–23. CrossRef Medline

Murakami T, Kondo S, Ogata M, Kanemoto S, Saito A, Wanaka A, Imaizumi K (2006) Cleavage of the membrane-bound transcription factor OASIS in response to endoplasmic reticulum stress. J Neurochem 96:1090–1100. CrossRef Medline

Murakami T, Saito A, Hino S, Kondo S, Kanemoto S, Chihara K, Sekiya H, Tsumagari K, Ochiai K, Yoshinaga K, Saitoh M, Nishimura R, Yoneda T, Kou I, Furuichi T, Ikegawa S, Ikawa M, Okabe M, Wanaka A, Imaizumi K (2009) Signalling mediated by the endoplasmic reticulum stress transducer OASIS is involved in bone formation. Nat Cell Biol 11:1205–1211. CrossRef Medline

Murphy D, Carter D (1990) Vasopressin gene expression in the rodent hypothalamus: transcriptional and posttranscriptional responses to physiological stimulation. Mol Endocrinol 4:1051–1059. CrossRef Medline

Mutsuga N, Shahar T, Verbalis JG, Xiang CC, Brownstein MJ, Gainer H (2005) Regulation of gene expression in magnocellular neurons in rat supraoptic nucleus during sustained hypoosmolality. Endocrinology 146:1254–1267. Medline

Noguchi T, Makino S, Matsumoto R, Nakayama S, Nishiyama M, Terada Y, Hashimoto K (2010) Regulation of glucocorticoid receptor transcription and nuclear translocation during single and repeated immobilization stress. Endocrinology 151:4344–4355. CrossRef Medline

Omori Y, Imai J, Suzuki Y, Watanabe S, Tanigami A, Sugano S (2002) OASIS is a transcriptional activator of CREB/ATF family with a transmembrane domain. Biochem Biophys Res Commun 293:470–477. CrossRef Medline

Panyasrivanit M, Greenwood MP, Murphy D, Isidoro C, Auewarakul P, Smith DR (2011) Induced autophagy reduces virus output in dengue infected monocytic cells. Virology 418:74–84. CrossRef Medline

Pardy K, Adan RA, Carter DA, Seah V, Burbach JP, Murphy D (1992) The identification of a cis-acting element involved in cyclic 3′,5′-adenosine monophosphate regulation of bovine vasopressin gene expression. J Biol Chem 267:21746–21752. Medline

Ponzio TA, Fields RL, Rashid OM, Salinas YD, Lubelski D, Gainer H (2012) Cell-type specific expression of the vasopressin gene analyzed by AAV mediated gene delivery of promoter deletion constructs into the rat SON in vivo. PLoS One 7:e48860. CrossRef Medline

Qiu J, Yao S, Hindmarch C, Antunes V, Paton J, Murphy D (2007) Transcription factor expression in the hypothalamo-neurohypophyseal system of the dehydrated rat: upregulation of gonadotrophin inducible transcription factor 1 mRNA is mediated by cAMP-dependent protein kinase A. J Neurosci 27:2196–2203. CrossRef Medline

Ray PE, Castrén E, Ruley EJ, Saavedra JM (1991) Different effects of chronic Na+, Cl−, and K+ depletion on brain vasopressin mRNA and plasma vasopressin in young rats. Cell Mol Neurobiol 11:277–287. CrossRef Medline

Saito A, Kanemoto S, Kawasaki N, Asada R, Iwamoto H, Oki M, Miyagi H, Izumi S, Sanosaka T, Nakashima K, Imaizumi K (2012) Unfolded protein response, activated by OASIS family transcription factors, promotes astrocyte differentiation. Nat Commun 3:967. CrossRef Medline

Salm AK, Hawrylak N (2004) Glial limitans elasticity subjacent to the supraoptic nucleus. J Neuroendocrinol 16:661–668. CrossRef Medline

Shiromani PJ, Magner M, Winston S, Charness ME (1995) Time course of phosphorylated CREB and Fos-like immunoreactivity in the hypothalamic supraoptic nucleus after salt loading. Brain Res Mol Brain Res 29:163–171. CrossRef Medline

Stewart L, Hindmarch CC, Qiu J, Tung YC, Yeo GS, Murphy D (2011) Hypothalamic transcriptome plasticity in two rodent species reveals divergent differential gene expression but conserved pathways. J Neuroendocrinol 23:177–185. CrossRef Medline

Uhl GR, Reppert SM (1986) Suprachiasmatic nucleus vasopressin messenger RNA: circadian variation in normal and Brattleboro rats. Science 232:390–393. CrossRef Medline

Yue C, Mutsuga N, Scordalakes EM, Gainer H (2006a) Studies of oxytocin and vasopressin gene expression in the rat hypothalamus using exon- and intron-specific probes. Am J Physiol Regul Integr Comp Physiol 290:R1233–R1241. CrossRef Medline

Yue C, Mutsuga N, Verbalis J, Gainer H (2006b) Microarray analysis of gene expression in the supraoptic nucleus of normoosmotic and hypoosmotic rats. Cell Mol Neurobiol 26:959–978. CrossRef Medline